

Theory of metasurface based perfect absorbers

Rasoul Alaei,^{*1,2} Mohammad Albooyeh³, Carsten Rockstuhl^{1,4}

¹*Institute of Theoretical Solid State Physics, Karlsruhe Institute of Technology, 76131 Karlsruhe, Germany*

²*Max Planck Institute for the Science of Light, Erlangen 91058, Germany*

³*Department of Electrical Engineering and Computer Science, University of California, Irvine, California 92697, USA*

⁴*Institute of Nanotechnology, Karlsruhe Institute of Technology, 76021 Karlsruhe, Germany*

**Corresponding author: rasoul.alaei@mpl.mpg.de*

Based on an analytic approach, we present a theoretical review on the absorption, scattering, and extinction of both dipole scatterers and regular arrays composed of such scatterers i.e., metasurfaces. Besides offering a tutorial by outlining the maximum absorption limit for electrically/magnetically resonant dipole particles/met-surfaces, we give an educative analytical approach to their analysis. Moreover, we put forward the analysis of two known alternatives in providing perfect absorbers out of electrically and or magnetically resonant metasurfaces; one is based on the simultaneous presence of both electric and magnetic responses in so called Huygens metasurfaces while the other is established upon the presence of a back reflector in so called Salisbury absorbers. Our work is supported by several numerical examples to clarify the discussions in each stage.

I. INTRODUCTION

Light carries energy. In many applications, e.g. optical sensors, thermal emitters, optical modulators, or solar cells, it is desirable to absorb as much as possible the energy of the impinging light in some absorbing layers. This requires to fully suppress the transmission and reflection while the energy shall be dissipated in the absorbing layer. In principle, perfect absorption occurs if two conditions are simultaneously satisfied: i.e., zero reflection and zero transmission. The first condition requires the absorbing layer (which can be, e.g., an electrically resonant layer) to be impedance matched to the free space. This fully suppresses the reflection. In order to satisfy the second condition (i.e. zero transmission), there are several approaches. For example we may choose the absorbing layer to be sufficiently thick (compared to the wavelength) or we may use several layers to create electromagnetic responses with both electric and magnetic properties.

Research studies on how electromagnetic waves can be efficiently absorbed potentially started with the invention of radar in the 1930's. At that time, it was important to disguise an object (e.g. an airplane) from radars. Therefore, various approaches have been introduced to reduce the reflected waves from the object¹. The most important inventions among them are Dallenbach² and Salisbury perfect absorbers³. Dallenbach perfect absorbers consist of a homogeneous lossy dielectric layer on top of a metallic ground plate [Fig. 1 (a)]. The thickness of the layer and its material properties (permittivity and permeability) have to be carefully chosen such that the reflected light is totally suppressed via impedance matching. The thickness of the layer should be roughly a quarter wavelength. In contrast, a Salisbury perfect absorber consists of a resistive sheet on top of a metallic ground plate separated by a dielectric spacer (no Ohmic losses) [Fig. 1 (b)]. This perfect absorber mainly relies on the absorption in the resistive sheet. The refractive index of the dielectric

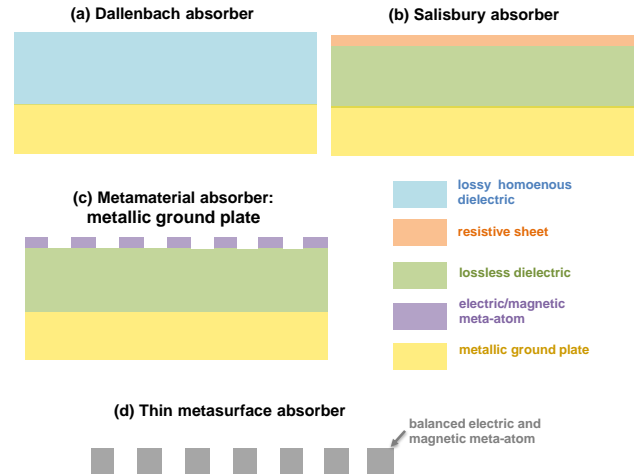


FIG. 1: Schematic view of three well-known perfect absorbers: (a) The Dallenbach perfect absorber, (b) the Salisbury perfect absorber, (c) the metamaterial perfect absorber made of electric/magnetic metasurface on top of a metallic ground plate, and (d) the thin metasurface perfect absorber made of balanced electric and magnetic meta-atoms.

spacer plays an important role on choosing the thickness of the layer. The basic principle of the Salisbury perfect absorbers can be understood by a destructive interference of the reflected light and a suppression of the transmitted light.

Recently, perfect metamaterial/met-surface absorbers [Fig. 1 (c)-(d)] have been introduced based on periodic subwavelength resonant particles (sometimes called meta-atoms or nanoantennas)^{4,5}. Perfect metamaterial absorbers attracted considerable attentions at microwave⁵⁻⁷, terahertz, and especially near-infrared⁸⁻¹³, and visible¹⁴⁻¹⁸ frequencies.

To understand the underlying physics of the metasurface based perfect absorbers, it is very important to ex-

plore the scattering properties of an individual element of such metasurfaces, usually referred as nanoantenna. For most pertinent nanoantennas the optical response can be fully described by an electric and/or magnetic dipole moment. An important question in this regard, therefore, would be: Is there any universal limitation on the scattering, absorption, and extinction properties of a nanoantenna which exhibits electric/magnetic dipole response? Moreover, it is important to have an analytical approach available to predict the optical response of an array of nanoantennas based on the response of the individual nanoantenna. By having this analytical approach, further questions one might ask are: What is the maximal achievable absorption for a metasurface, which exhibit only an electric/magnetic response? Finally, is it possible to achieve complete light absorption for an array of dipole resonant scatterers? In this paper, we try to answer all the aforementioned questions by a theoretical review on the limits of absorption and scattering of both an individual dipole resonant scatterer and a condense array of such resonant scatterers i.e., metasurfaces¹⁹. We support our theoretical review by adapted numerical simulations when required. Even though partially already documented in literature, these insights have not yet been presented in a concise manner. It is the purpose of this contribution to close this gap.

II. SCATTERING PROPERTIES OF NANOANTENNAS: UNIVERSAL LIMITATIONS

Nanoantennas are canonical elements in nanooptics, which control light-matter interaction at the nanoscale. Nanoantennas are usually made of two types of materials i.e. a) metals or b) dielectrics. In the case of metals, nanoantennas support a localized surface plasmon polariton resonance. This is a collective oscillation of the conduction electrons of the metallic antenna resonantly coupled to the electromagnetic wave at visible or near-infrared frequencies²⁰. In the case of dielectric nanoantennas, Mie resonances are excited, which are also known as whispering gallery resonances. In this section, we want to review some universal limitations (in the dipole approximation) on their interaction with light^{21,23-27}.

A. Electric dipole

Let us start with the simplest case, i.e. a nanoantenna that only supports an electric dipole moment \mathbf{p} . We start by considering an incident plane wave with an electric field E_x^{inc} polarized along the x -axis that propagates in z -direction. The induced electric dipole moment p_x in the nanoantenna is expressed as²¹

$$p_x = \epsilon_0 \alpha_{ee} E_x^{\text{inc}},$$

where α_{ee} is the electric polarizability (here, we assumed an isotropic and electric dipolar particle so that α_{ee} is a

scalar) and ϵ_0 is the free space permittivity. The scattered electric \mathbf{E}_{sca} and magnetic \mathbf{H}_{sca} far-fields by the induced electric dipole moment p_x are given by²⁸

$$\begin{aligned} \mathbf{E}_{\text{sca}} &= Z_0 \mathbf{H}_{\text{sca}} \times \mathbf{n} = \frac{ck^2}{4\pi} Z_0 (\mathbf{n} \times \mathbf{p}) \times \mathbf{n} \frac{e^{ikr}}{r}, \\ \mathbf{H}_{\text{sca}} &= \frac{ck^2}{4\pi} (\mathbf{n} \times \mathbf{p}) \frac{e^{ikr}}{r}, \end{aligned} \quad (1)$$

where \mathbf{n} is the normal unit vector along the radial direction of the Spherical Coordinates, Z_0 is the impedance of the ambient material, $k = \omega/c$ is the wavenumber for an angular frequency ω in vacuum, and c is the speed of light in vacuum. The exponential dependence of the fields on the spatial coordinate and the frequency is omitted here for brevity. By using the above expressions, the scattered (or radiated) power (i.e. the surface integral of the outward flowing flux of the Poynting vector of scattered fields) of the induced electric dipole moment reads (see the Appendix)

$$\begin{aligned} P_{\text{sca}} &= \frac{1}{2} \text{Re} \iint_S (\mathbf{E}_{\text{sca}} \times \mathbf{H}_{\text{sca}}^*) \cdot \mathbf{n} \, ds \\ &= \frac{c^2 Z_0 k^4}{12\pi} |\mathbf{p}|^2 = \frac{k^4}{6\pi} |\alpha_{ee}|^2 \frac{|E_x^{\text{inc}}|^2}{2Z_0}. \end{aligned} \quad (2)$$

Now by using the definition of the time-averaged Poynting vector for the illuminating plane wave, by defining the intensity of the impinging light as $I_0 = \frac{1}{2} \text{Re} (\mathbf{E}_{\text{inc}} \times \mathbf{H}_{\text{inc}}^*) = |E_x^{\text{inc}}|^2 / 2Z_0$, and by using Eq. 2, the total scattering cross section of the induced electric dipole moment is expressed as

$$C_{\text{sca}} = \frac{P_{\text{sca}}}{I_0} = \frac{k^4}{6\pi} |\alpha_{ee}|^2. \quad (3)$$

On the other hand, the extracted power is defined as²⁹ (see the Appendix)

$$\begin{aligned} P_{\text{ext}} &= -\frac{1}{2} \text{Re} \iint_S (\mathbf{E}_{\text{inc}} \times \mathbf{H}_{\text{sca}}^* + \mathbf{E}_{\text{sca}} \times \mathbf{H}_{\text{inc}}^*) \cdot \mathbf{n} \, ds \\ &= -\frac{\omega}{2} \text{Im} (\mathbf{p}^* \cdot \mathbf{E}_{\text{inc}}) = \frac{1}{2} \omega \epsilon_0 \alpha_{ee}'' |\mathbf{E}_{\text{inc}}|^2, \end{aligned} \quad (4)$$

where α_{ee}'' is the imaginary part of the electric polarizability. Similar to scattering, the extinction cross section is defined as $C_{\text{ext}} = \frac{P_{\text{ext}}}{I_0} = k \text{Im} (\alpha_{ee}) = k \alpha_{ee}''$. It is well-known that the extracted power is the sum of the scattered power P_{sca} and the absorbed power P_{abs} i.e., $P_{\text{ext}} = P_{\text{sca}} + P_{\text{abs}}$ ²⁹. The same is valid for the cross sections, i.e. $C_{\text{ext}} = C_{\text{sca}} + C_{\text{abs}}$. Therefore, the absorption cross section reads

$$\begin{aligned} C_{\text{abs}} &= \frac{P_{\text{abs}}}{I_0} = \frac{P_{\text{ext}} - P_{\text{sca}}}{I_0} \\ &= k \alpha_{ee}'' - \frac{k^4}{6\pi} |\alpha_{ee}|^2. \end{aligned} \quad (5)$$

Now we can calculate the maximum possible absorption cross section by differentiating C_{abs} with respect to the real and imaginary parts of the polarizability, i.e. α'_{ee} and α''_{ee} and the results read $\alpha'_{ee} = 0$, $\alpha''_{ee} = 3\pi/k^3$. This suggests that in order to achieve a maximal absorption cross section, the nanoantenna should be in resonance, i.e. the real part of the polarizability should be zero. By substituting $\alpha'_{ee} = 0$, $\alpha''_{ee} = 3\pi/k^3$ into Eq. 5, the maximum absorption cross section reads $C_{\text{abs}}^{\text{max}} = \frac{3\pi}{2k^2} = \frac{3}{8\pi}\lambda^2$. At the same time, the scattering cross section is $C_{\text{sca}} = \frac{3\pi}{2k^2}$. Therefore, we can conclude that a nanoantenna which exhibits only an electric dipole response is most absorptive if the absorbed power is identical to its scattered power, i.e. $C_{\text{abs}}^{\text{max}} = C_{\text{sca}} = \frac{3\pi}{2k^2}$. This condition is known as *critical coupling*^{14,26,30,31}. Moreover, it is important to mention that for such a nanoantenna the scattering/absorption cross section ($C_{\text{abs}}^{\text{max}}$ or C_{sca}) can exceed the geometrical cross section (A) by an order of magnitude. To exemplify it, let us assume a nanodisk antenna with a finite height, radius a and geometrical cross section of $A = \pi a^2$. The nanoantenna shall be sufficiently small compared to the wavelength ($ka \ll 1$). Hence, the absorption/scattering cross section can be much bigger than the geometrical cross section at critical coupling, i.e.

$$\frac{C_{\text{sca}}}{A} = \frac{C_{\text{abs}}^{\text{max}}}{A} = \frac{3}{2(ka)^2} \gg 1. \quad (6)$$

Note that for metallic nanoantennas the enhanced absorption is associated with the excitation of surface plasmon polaritons²⁰, which leads to a huge near-field enhancement. This field enhancement will play a crucial rule to achieve promising applications in quantum optics and optical sensing. For lossy dielectric nanoantennas at infrared wavelengths the absorption is associated with the excitation of phonons³².

To gain further insights into the scattering response, let us study the implications of the analysis above to some limiting cases. For that, let us focus on a scatterer made of a non-absorbing material. It implies that the absorbed power is zero ($P_{\text{abs}} = 0$). This means that the impinging energy of the illuminating plane wave on the nanoantenna will be entirely scattered into the surrounding media. Therefore, the extracted and scattered power should be identical, i.e. $P_{\text{ext}} = P_{\text{sca}}$. This equality leads to a well-known expression for the imaginary part of the polarizability

$$\text{Im}\left(\frac{1}{\alpha_{ee}}\right) = -\frac{\alpha''_{ee}}{|\alpha_{ee}|^2} = -\frac{k^3}{6\pi}. \quad (7)$$

Equation 7 presents an important physical quantity that is known as the *scattering losses*; also called *radiation losses*^{21,33}. Note that this quantity only depends on the wavelength and is independent of the geometrical parameters and materials that the nanoantenna is made of.

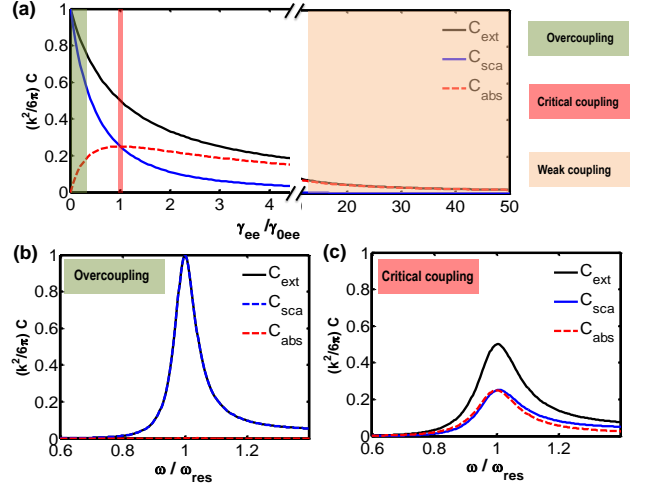


FIG. 2: (a) Normalized extinction, absorption, and scattering cross sections at resonance as a function of the normalized Ohmic losses (i.e. γ_{ee}/γ_{ee0}). (b) Normalized extinction, absorption, and scattering cross sections as a function of the normalized frequency for the lossless case (i.e. $\gamma_{ee} = 0$). (c) The same plot as (b) but for the case of maximum absorption cross section or critical coupling (i.e. $\gamma_{ee} = \gamma_{ee0}$).

Next, let us assume that the nanoantenna is made of a lossy material. In order to contextualize the aforementioned results, let us assume that the polarizability of the nanoantenna α_{ee} can be expressed by a Lorentzian line-shape that reads as^{15,33}

$$\alpha_{ee} = \frac{\alpha_{0ee}}{\omega_{0ee}^2 - \omega^2 - i\omega\gamma_{ee} - i\frac{k^3}{6\pi}\alpha_{0ee}}, \quad (8)$$

where ω_{0ee} is the resonance frequency, γ_{ee} is expressing the Ohmic losses (also called nonradiative losses), and α_{0ee} is the strength of resonance. The last term, i.e. $\frac{k^3}{6\pi}$, is related to the scattering losses. Note that Eq. 8 fulfils Eq. 7 if the Ohmic losses are zero, i.e. $\gamma_{ee} = 0$.

By using Eqs. 3, 4, and 7, the scattering and extinction cross sections are given by

$$C_{\text{sca}} = \frac{k^4}{6\pi} \frac{\alpha_{0ee}^2}{(\omega_{0ee}^2 - \omega^2)^2 + (\omega\gamma_{ee} + \frac{k^3}{6\pi}\alpha_{0ee})^2}, \quad (9)$$

$$C_{\text{ext}} = \frac{k\alpha_{0ee} \left(\omega\gamma_{ee} + \frac{k^3}{6\pi}\alpha_{0ee} \right)}{(\omega_{0ee}^2 - \omega^2)^2 + (\omega\gamma_{ee} + \frac{k^3}{6\pi}\alpha_{0ee})^2}. \quad (10)$$

We calculated the scattering, absorption, and extinction cross sections as a function of the normalized Ohmic losses at the resonance frequency [Fig. 2 (a)]. They are normalized to $\frac{6\pi}{k^2}$, which is the maximum extinction cross section. Moreover, the Ohmic losses are normalized to the scattering losses. In principle, three different coupling regimes are distinguished:

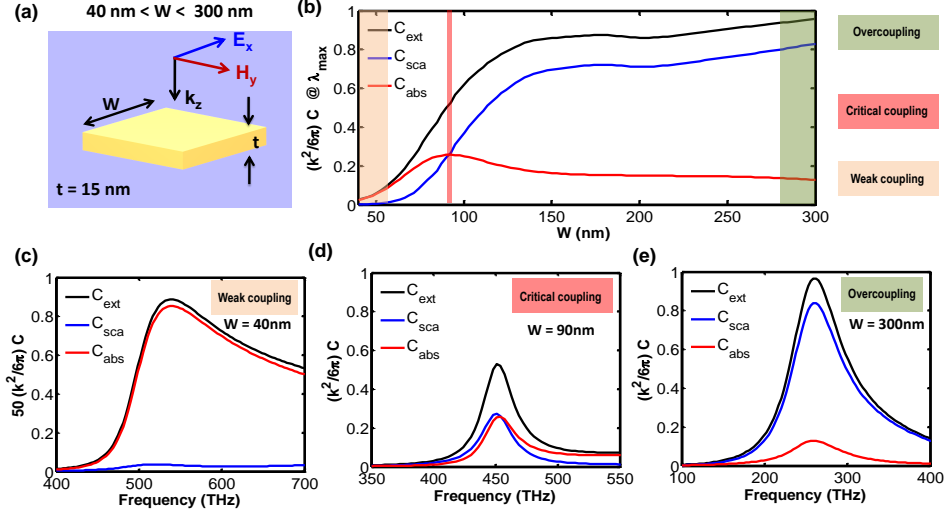


FIG. 3: (a) Schematic of the considered nanopatch antenna. (b) Normalized extinction, scattering, absorption cross sections at resonance frequency (λ_{max}) as a function of the width of the investigated nanopatch nanoantenna (i.e. W). (c) Normalized extinction, scattering, absorption cross sections as a function of frequency when the width of the nanoantenna is $W = 40$ nm. In this case the $C_{\text{ext}} \approx C_{\text{abs}}$. This occurs for nanoantennas really small compared to the wavelength. (d) Same as (c) whenever the nanoantenna is at critical coupling, i.e. $C_{\text{abs}}|_{\lambda_{\text{max}}} = C_{\text{ext}}|_{\lambda_{\text{max}}}$. This occurs if the width of nanoantenna is $W = 90$ nm. (e) Same as (c) when the scattering cross section dominates, here at $W = 300$ nm. Note that by using induced electric current, it is easy to show that the considered nanopatch antenna only supports an electric dipole moment³⁴.

a) *Overcoupling* ($\gamma_{ee} \ll \gamma_{0ee}$): This occurs if the Ohmic losses (i.e. γ_{ee}) of the nanoantenna are much smaller than the scattering losses (i.e. γ_{0ee}). The scattering losses are defined as $\gamma_{0ee} = \frac{k^3}{6\pi} \left(\frac{\alpha_{0ee}}{\omega_0} \right)$. Figure 2 (b) shows the normalized scattering, absorption, and extinction cross sections as a function of the normalized frequency (i.e. $\omega/\omega_{\text{res}}$) for the lossless case, i.e. $\gamma_{ee} = 0$. It can be seen that the scattering and extinction cross sections are identical, i.e. $C_{\text{ext}} = C_{\text{sca}}$.

b) *Critical coupling* ($\gamma_{ee} = \gamma_{0ee}$): This occurs whenever the Ohmic losses (γ_{ee}) are identical to the scattering losses (γ_{0ee}). This condition allows to achieve maximum absorption. It can be seen that the maximum absorption cross section occurs whenever $\gamma_{ee} = \gamma_{0ee} = \frac{k^3}{6\pi} \left(\frac{\alpha_{0ee}}{\omega_0} \right)$ [Fig. 2 (a) and (c)]. Figure 2 (c) shows the same plot as Fig. 2 (b) for the case of critical coupling. In this case, the absorption cross section is identical to the scattering cross section, i.e. $C_{\text{abs}} = C_{\text{sca}}$. Therefore, the extinction cross section will be $C_{\text{ext}} = 2C_{\text{abs}} = 2C_{\text{sca}}$.

c) *Weak coupling* ($\gamma_{ee} \gg \gamma_{0ee}$): This occurs if the Ohmic losses (γ_{ee}) are much larger than the scattering losses (γ_{0ee}). At extremely large Ohmic losses, i.e. $\gamma_{ee} \gg \gamma_{0ee}$, the scattering cross section is considerably small with respect to the absorption cross section, i.e. $C_{\text{sca}} \ll C_{\text{abs}}$. In other words, the absorption cross section is approximately identical to the extinction cross section, i.e. $C_{\text{ext}} \approx C_{\text{abs}}$. This occurs whenever the nanoantenna is considerably small with respect to the wavelength or the dissipative losses of nanoantenna material is too high. The frequency dependency of the scattering, absorption, and extinction cross sections for the

weak coupling regime is not shown here.

The aforementioned theoretical results can be applied to an arbitrary plasmonic nanoantenna as long as it supports *only* an electric dipole response. In order to confirm that, we investigate possibly the simplest nanoantenna, i.e. a gold nanopatch [Fig. 3 (a)]. The permittivity of gold is taken from Ref. 35. We used a numerical finite element solver to obtain all the numerical results³⁶. The height of the nanopatch is assumed to be $t = 15$ nm and its width W is varying from 40 nm to 300 nm. It can be seen that by varying the width W of the nanoantenna, it is possible to tune the Ohmic losses. This is shown in Fig. 3 (a). For small nanoantennas, i.e. $W < 60$ nm, the absorption cross section is much larger than the scattering cross section, i.e. $C_{\text{abs}} \approx C_{\text{ext}}$ [Fig. 3 (c)]. In principle, this is always valid for a nanoantenna much smaller than the operating wavelength. By increasing the width of the nanopatch, the condition for critical coupling (maximum absorption regime) is met. In the chosen example this happens for $W = 90$ nm [Fig. 3(c)]. Finally, for considerably large nanoantenna, scattering losses dominate and the extinction cross section might reach its maximum value, i.e. $C_{\text{ext}} = \frac{6\pi}{k^2} = \frac{3\lambda^2}{2\pi}$. In other words, the absorption cross section is small compared to the scattering cross section, i.e. $C_{\text{ext}} \approx C_{\text{sca}} \gg C_{\text{abs}}$.

All the results in this subsection are equally valid when considering a nanoantenna that supports a magnetic dipole moment (see e.g. Refs. 37–39). All the equations for a magnetic dipole moment are analogous, or dual, to those for an electric dipole moment. In fact, this can be understood from the duality of the electric and magnetic fields/currents in Maxwell's equations. A similar expres-

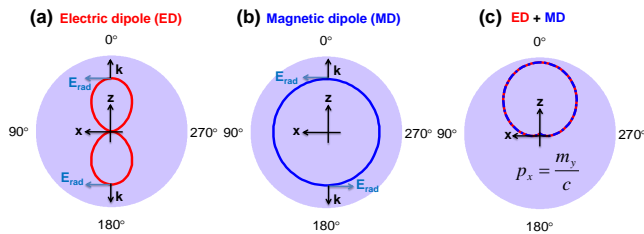


FIG. 4: Radiation pattern for different multipole moments in the xz -plane. (a) Electric dipole moment (p_x), i.e. $|\mathbf{E}_{\text{far}}|^2 \propto |p_x|^2 \cos^2 \theta$. The blue arrows indicate the phase of the radiated field. (b) Magnetic dipole moment (m_y), i.e. $|\mathbf{E}_{\text{far}}|^2 \propto |\frac{m_y}{c}|^2$. (c) Superposition of electric and magnetic dipole moments, i.e. $|\mathbf{E}_{\text{far}}|^2 \propto |p_x|^2 (1 + \cos \theta)^2$, when the Kerker condition is fulfilled, i.e. $p_x = \frac{m_y}{c}$.

sion to that of Eq. 7 also holds for the scattering losses of a magnetic dipole, i.e. $\text{Im}\left(\frac{1}{\alpha_{\text{mm}}}\right) = -\frac{k^3}{6\pi}$. This expression is called Sipe-Kranendonk condition that can be obtained from conservation of energy^{21,33,40}. Note that the above discussions are valid as long as the nanoantenna exhibits only an electric/magnetic dipole moment. It is also interesting to mention that these universal limitations are independent of the shape and material of the nanoantenna. Experimental verification of some of the above results can be found in⁴¹⁻⁴³.

B. Electric and magnetic dipoles and higher order multipoles

For a dipolar particle that simultaneously supports an electric and magnetic response represented, respectively, by electric and magnetic dipole moments p_x and m_y , the radiated electric far-field reads^{28,44}

$$\mathbf{E}_{\text{sca}}(\mathbf{r}) = \frac{k^2}{4\pi\epsilon_0} p_x \frac{e^{ikr}}{r} \left(-\sin\varphi \hat{\phi} + \cos\theta \cos\varphi \hat{\theta} \right) - \frac{k^2}{4\pi\epsilon_0} \frac{m_y}{c} \frac{e^{ikr}}{r} \left(\cos\theta \sin\varphi \hat{\phi} - \cos\varphi \hat{\theta} \right), \quad (11)$$

where, r is the distance to the observation point, ϕ is the azimuthal angle, and θ is the polar angle in spherical coordinates. The extinction and scattering cross sections, respectively, read

$$C_{\text{ext}} = C_{\text{ext}}^p + C_{\text{ext}}^m = k \text{Im}(\alpha_{\text{ee}} + \alpha_{\text{mm}}), \quad (12)$$

$$C_{\text{sca}} = \frac{k^4}{6\pi} (|\alpha_{\text{ee}}|^2 + |\alpha_{\text{mm}}|^2). \quad (13)$$

The maximum scattering cross section is $C_{\text{ext}} = 2\frac{3\lambda^2}{2\pi}$, which is two times larger than that of an individual electric or a magnetic dipole. This occurs if the antenna is in the overcoupling regime and the Kerker condition

$p_x = m_y/c$ is fulfilled ($C_{\text{ext}}^p = C_{\text{ext}}^m$). To illustrate the physical mechanism behind the Kerker condition, the radiation pattern of such dipole antenna in the xz -plane ($\varphi = 0$) is shown in Figs. 4 (a) and (b). The electric field radiated by an electric dipole and a magnetic dipole interfere constructively at $\theta = 0$ [Fig. 4 (c)], i.e. their radiated fields are in-phase in forward direction [Fig. 4 (a) and (b)]. On the other hand, there is no scattering in backward direction ($\theta = \pi$) because of the destructive interference in this direction. The maximum absorption cross section $C_{\text{abs}} = 2\frac{3}{8\pi}\lambda^2$ occurs at critical coupling.

For particles large compared to the wavelength, higher order multipole moments (e.g. quadrupole, octupole, etc.) will be excited. By applying the energy conservation principle, one can show that the maximum scattering/extinction cross section of an isotropic particle is $(2j+1)\lambda^2/2\pi^{24,31,45}$, where j is the total angular momentum number and $j = 1, 2, 3$, respectively, correspond to the electric/magnetic dipole, quadrupole, and octupole moments. Similarly, the maximum absorption cross section is $(2j+1)\lambda^2/8\pi^{24,31,45}$. These fundamental limits for the scattering, absorption and extinction cross sections lead to some upper bounds for optical force and torque⁴⁵.

III. OPTICAL PROPERTIES OF AN ARRAY OF ELECTRIC NANOANTENNAS

The interaction of light with a periodic array of optically small resonant nanoantennas (also called metasurfaces) is an interesting and fundamental problem which attracts tremendous interests⁴⁶⁻⁴⁸. In this section, we concisely study and present a summary on the limitations concerning the optical properties of such an array of nanoantennas. We assume that nanoantennas are optically small and the externally incidence field only excites electric dipole moments of nanoantennas. We show that a periodic array of electric dipoles maximally absorbs 50 percent of the impinging light.

Let us consider an infinite planar array of optically small resonant nanoantennas, which support only an electric dipole moment. The array is excited by a plane wave (normal incidence) with an electric field polarized along the x -axis that propagates in the positive z -direction [Fig. 5] so each dipole must be induced along the x -axis. We assume that the array of nanoantennas is situated in the xy -plane and embedded in a homogeneous lossless medium. The period Λ of the array is sufficiently small compared to the wavelength and $W \ll \lambda$ where W is a measure for the spatial extent of the individual nanoantenna. The shape of the nanoantennas can be arbitrary, e.g. nanopatches, nanodiscs, nanostrips, nanospheres, or nanocylinders. The only requirement is to have a nanoantenna topology to induce only a co-polarized electric dipole moment, i.e. p_x (without cross polarization), along the polarization of the incidence. All the higher order multipole moments should be negligible. Now, in

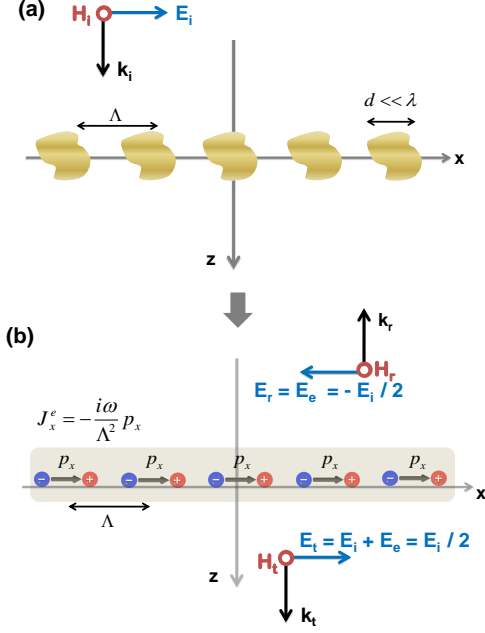


FIG. 5: (a) Geometry of an infinite periodic array of nanoantennas that support only an electric dipole moment. The array is embedded in a uniform homogeneous host medium and excited by a plane wave. The two-dimensional array is periodic in the x-y plane. (b) The radiated fields by the average electric current density J_x in the case of maximum absorption, i.e. $A_{\max} = 0.5$.

order to calculate the optical response of a periodic array of electric dipoles [Fig. 5 (b)], let us express the induced electric dipole moment p_x . It reads comparable to that of a sample nanoantenna as

$$p_x = \epsilon_0 \alpha_{ee} E_x^{\text{loc}}, \quad (14)$$

where E_x^{loc} is the local electric field at the dipole position and is defined as $E_x^{\text{loc}} = E_x^{\text{inc}} + E_x^{\text{int}}$. E_x^{inc} is the incident electric field and E_x^{int} is the interaction field created by the rest of the electric dipoles in the array at the position of the sample dipole²¹. The interaction field is proportional to p_x and can be expressed by $E_x^{\text{int}} = \frac{\beta_{ee} p_x}{\epsilon_0}$. Here, the interaction constant β_{ee} is given by^{21,49,50}

$$\beta_{ee} = \frac{ik}{4\Lambda^2} \left(1 + \frac{1}{ikR_0} \right) e^{ikR_0}, \quad (15)$$

where $R_0 = \Lambda/1.438$ is the effective inter-particle distance. This is calculated for the quasi-static case and it is a good approximation as long as the array is condense and the nanoantennas are small compared to the wavelength. Details about the derivation of the interaction constant β_{ee} can be found in Refs. 21,49,50. Note that the imaginary part of the interaction constant for a periodic array can be calculated without any approximation by using a conservation of energy²¹ and can be written

as

$$\text{Im}(\beta_{ee}) = \text{Im} \left(\frac{1}{\alpha_{ee}} \right) + \frac{k}{2\Lambda^2} = -\frac{k^3}{6\pi} + \frac{k}{2\Lambda^2}. \quad (16)$$

It is very important to notice that the first term in Eq. 16 cancels out with the scattering losses (i.e. $-\frac{k^3}{6\pi}$) in regular arrays and the second term (i.e. $\frac{k}{2\Lambda^2}$) is related to the plane wave contribution created by the induced averaged electric surface current. Finally, the interaction constant reads²¹

$$\begin{aligned} \beta_{ee} &= \text{Re}(\beta_{ee}) + i\text{Im}(\beta_{ee}) \\ &= \text{Re} \left[\frac{ik}{4\Lambda^2} \left(1 + \frac{1}{ikR_0} \right) e^{ikR_0} \right] + i \left(-\frac{k^3}{6\pi} + \frac{k}{2\Lambda^2} \right). \end{aligned} \quad (17)$$

By using Eq. 14 and the local field definition, the induced electric dipole moment reads²¹

$$p_x = \epsilon_0 \frac{\alpha_{ee}}{1 - \alpha_{ee}\beta_{ee}} E_x^{\text{inc}} = \epsilon_0 \alpha_{\text{eff}} E_x^{\text{inc}}, \quad (18)$$

where $\alpha_{\text{eff}} = \alpha_{ee} / (1 - \alpha_{ee}\beta_{ee})$ is the so-called effective or renormalized electric polarizability of the array. To calculate the reflection and transmission coefficients, we use the generalized boundary condition^{21,51-54}, i.e. $E_x^r = -\frac{1}{2} Z_0 J_x$ and the induced averaged electric surface current density, i.e. $J_x^e = -i\omega \frac{p_x}{\Lambda^2}$. Note that the average magnetic surface current is zero. Therefore, the reflected electric field is given as

$$\begin{aligned} E_x^r &= -\frac{1}{2} Z_0 J_x^e = \frac{i\omega}{2\Lambda^2} Z_0 p_x \\ &= \frac{ik}{2\Lambda^2} \frac{\alpha_{ee}}{1 - \alpha_{ee}\beta_{ee}} E_x^{\text{inc}}, \end{aligned} \quad (19)$$

and finally the reflection and transmission coefficients reads

$$r = \frac{E_x^r}{E_x^{\text{inc}}} = \frac{ik}{2\Lambda^2} \frac{\alpha_{ee}}{1 - \alpha_{ee}\beta_{ee}}, \quad (20)$$

$$t = \frac{E_x^t}{E_x^{\text{inc}}} = 1 + \frac{ik}{2\Lambda^2} \frac{\alpha_{ee}}{1 - \alpha_{ee}\beta_{ee}}. \quad (21)$$

Equations 20 and 21 hold only for an optically thin layer of nanoantennas. The absorption is calculated from the reflection and transmission coefficients and reads $A = 1 - |r|^2 - |t|^2$. The reflection coefficient is a complex number and can be written as $r = r_r + ir_i$. Here, r_r is the real part and r_i is the imaginary part of the complex reflection coefficient r . Thus, the absorption in terms of real and imaginary parts of the reflection coefficient can be written as $A = -2(1 + r_r)r_r - 2r_i^2$. Now, we can find the condition for maximum absorption for an array that supports only electric dipole moments by differentiating the absorption A with respect to r_r and r_i and searching for the roots, identifying extremal points in the absorption, i.e. $r_r = -\frac{1}{2}$, $r_i = 0$. From that analysis it turns out that in order to obtain maximum absorption, the reflection and transmission coefficients of the array should

be $r = -\frac{1}{2}$, $t = 1 + r = \frac{1}{2}$. By substituting these values of r and t into $A = 1 - |r|^2 - |1 + r|^2$, one can see that an array of resonant electric dipoles maximally absorbs 50 percent of the impinging light, i.e. $A_{\max} = \frac{1}{2}$. This is a universal limitation that holds for periodic arrays as long as it supports only an electric response. In order to cancel the incident field, the array of electric dipoles should radiate a plane wave with the same amplitude in both forward and backward directions. The optimum case occurs when only half of the incident field is canceled as shown in Fig. 5. In the case of the maximum absorption, the induced averaged electric surface current density will be $J_x^e = \frac{E_x^{\text{inc}}}{Z}$. The corresponding individual polarizability is given by

$$\alpha_{ee} = \frac{1}{\beta_{ee} - \frac{ik}{\Lambda^2}}. \quad (22)$$

For a dense array of lossless (no Ohmic losses) nanoantennas, it can be easily shown that the reflection coefficient at resonance will reach $r = -1$. Therefore, the transmission coefficient necessarily has to be zero $t = 1 + r = 0$. As a result, the corresponding individual polarizability can be expressed as

$$\alpha_{ee} = \frac{1}{\beta_{ee} - \frac{ik}{2\Lambda^2}}. \quad (23)$$

In order to quantitatively understand the fundamental limitation of absorption for an array of electric dipole moments, let us now assume that the polarizability of an individual nanoantenna possesses a Lorentzian line-shape given by Eq. 8. By using Eq. 20 and the inter-particle interaction constant, i.e. $\beta_{ee} = \text{Re}(\beta_{ee}) - i\frac{k^3}{6\pi} + i\frac{k}{2\Lambda^2}$ ²¹, the reflection coefficient reads

$$r = \frac{ik}{2\Lambda^2} \frac{\alpha_{0ee}}{\omega_0'^2 - \omega^2 - i\omega \left(\gamma_{ee} + \frac{\alpha_0}{2\Lambda^2 c_0} \right)}, \quad (24)$$

where $\omega_0' = \omega_0 - \text{Re}(\beta_{ee})\alpha_{0ee}$ is the resonance frequency of the array, which is shifted compared to the resonance of an individual nanoantenna (i.e. ω_0). The reflection coefficient at the resonance frequency $\omega = \omega_0'$ is given by

$$r(\omega = \omega_0') = -\frac{\frac{\alpha_0}{2\Lambda^2 c_0}}{\left(\gamma_{ee} + \frac{\alpha_0}{2\Lambda^2 c_0} \right)} = -\frac{\gamma_{0ee}}{(\gamma_{ee} + \gamma_{0ee})}, \quad (25)$$

where $\gamma_{0ee} = \frac{\alpha_0}{2\Lambda^2 c_0}$ while the transmission coefficient will be $t(\omega = \omega_0') = 1 + r(\omega = \omega_0') = \gamma_{ee}/(\gamma_{ee} + \gamma_{0ee})$.

To better understand all the aforementioned results, the reflection, transmission, and absorption of an array of electric dipoles at the resonance frequency as a function of the normalized dissipation losses (i.e. γ_{ee}/γ_{0ee}) are shown in Fig. 6 (a). It can be seen that the maximum reflection (i.e. $R_{\max} = |r_{\max}|^2 = 1$, $r_{\max} = -1$) occurs if the nanoantennas in the array are lossless, i.e.

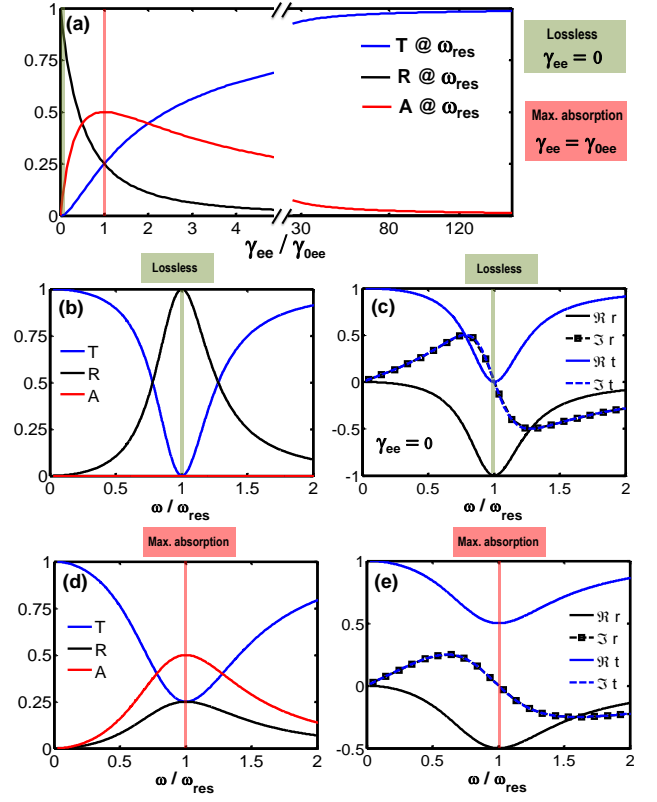


FIG. 6: (a) Transmission, reflection, and absorption at resonance frequency as a function of normalized dissipation losses (i.e. γ_{ee}/γ_{0ee}). Maximum absorption (i.e. $A_{\max} = 0.5$) occurs whenever $\gamma_{ee} = \gamma_{0ee}$ (red line). (b) The transmission, reflection, and absorption as a function of normalized frequency for the lossless case, i.e. $\gamma_{ee} = 0$. (c) The same plot as (b) for the reflection and transmission coefficients. (d)-(e) Same plots as (b) and (c) for the case of maximal absorption (i.e. $\gamma_{ee} = \gamma_{0ee}$).

$\gamma_{ee} = 0$ [Fig. 6 (a)-(c)]. The transmission ($t = 1 + r$) for such a lossless array goes to zero at resonance frequency [Fig. 6 (b) and (c)]. The array achieves its maximum absorption, i.e. $A_{\max} = \frac{1}{2}$, if the dissipation loss is equal to $\gamma_{ee} = \gamma_{0ee} = \frac{\alpha_0}{2\Lambda^2 c_0}$. This point of operation is shown with red line in Fig. 6 (a) and (d). In this case, the reflection and transmission coefficients will be $r = -1/2$ and $t = 1/2$, which can easily be seen in Fig. 6 (e).

As a practical example, we investigate an array of gold nanopatches which exhibits only an electric dipolar response. It is possible to achieve the maximal absorption for the array by proper varying the geometrical parameters of the nanopatches and the periodicity such that it satisfies Eq. 22. This is shown in Fig. 7 (b). Note that the results [Figs. 7 (b) and (c)] are in good agreement with the analytical findings explained in the previous chapter [Figs. 6 (d) and (e)].

Finally, due to the duality, the response of an array of magnetic dipoles is similar to the electric one. Therefore, it is important to highlight that an array of magnetic

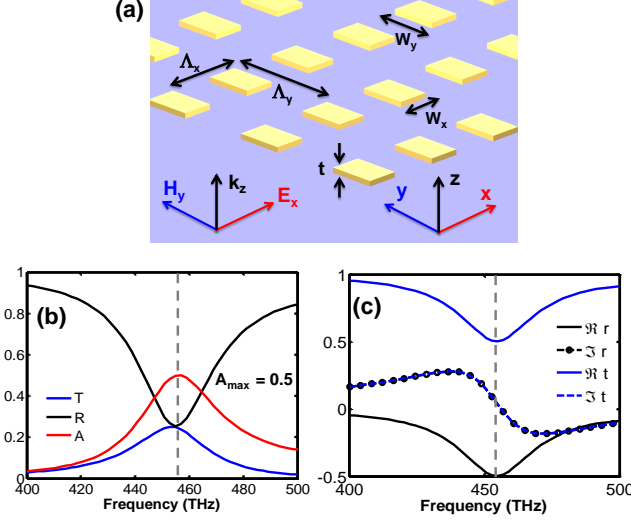


FIG. 7: (a) Schematic view of the rectangular nanopatches designed for maximum absorption, i.e. $A_{\max} = \frac{1}{2}$. (b) The reflection, transmission and absorption spectra. (c) The reflection and transmission coefficients. Note that at resonance, $r|_{\text{res}} = -\frac{1}{2}$ and $t|_{\text{res}} = \frac{1}{2}$. The period in x and y directions are $\Lambda_x = 320$ nm and $\Lambda_y = 500$ nm. The gold nanopatch has a thickness of $t = 15$ nm and a width of $W_x = 100$ nm and $W_y = 145$ nm.

dipoles maximally absorbs 50 percent of impinging light.

We have so far presented a summary of maximum possible absorption of an electrically or a magnetically resonant array of dipole nanoantennas. However, there are several approaches to increase the absorption in such arrays which, in some cases, even allows to achieve full absorption. One method is to take the advantage of dipole nanoantennas that simultaneously support both electric and magnetic responses, as discussed in Refs. 5,37,55,56. In the next section, we theoretically review this problem.

IV. OPTICAL PROPERTIES OF AN ARRAY OF ELECTRIC AND MAGNETIC NANOANTENNAS

Let us assume that an array of electric and magnetic dipole particles is located in the xy -plane and is illuminated by a plane wave with an electric field polarized along the x -axis that propagates in the positive z -direction (Fig. 8). The period of the array is Λ , which is considered to be sufficiently small compared to the wavelength λ . The constitutive relations between the induced dipole moments (p_x, m_y) and local fields ($E_x^{\text{loc}}, H_y^{\text{loc}}$) read

$$\begin{aligned} p_x &= \epsilon_0 \alpha_{ee} E_x^{\text{loc}}, \\ m_y &= \alpha_{mm} H_y^{\text{loc}}, \end{aligned}$$

where $E_x^{\text{loc}} = E_x^{\text{inc}} + E_x^{\text{int}}$ and $H_y^{\text{loc}} = H_y^{\text{inc}} + H_y^{\text{int}}$. By using the generalized boundary conditions and the averaged electric and magnetic current densities^{21,51-54}, we

write the reflected E_x^r and transmitted E_x^t electric fields in terms of the electric and magnetic dipole moments as

$$E_x^r = \frac{i\omega}{2\Lambda^2} (Z_0 p_x - \mu_0 m_y), \quad (26)$$

$$E_x^t = E_x^{\text{inc}} + \frac{i\omega}{2\Lambda^2} (Z_0 p_x + \mu_0 m_y). \quad (27)$$

Next, by employing the relation between the local and incident fields, we obtain the dipole moments in terms of the incident fields, i.e.,

$$p_x = \epsilon_0 \frac{\alpha_{ee}}{1 - \alpha_{ee}\beta_{ee}} E_x^{\text{inc}} = \epsilon_0 \alpha_{ee}^{\text{eff}} E_x^{\text{inc}}, \quad (28)$$

$$m_y = \frac{\alpha_{mm}}{1 - \alpha_{mm}\beta_{mm}} H_y^{\text{inc}} = \alpha_{mm}^{\text{eff}} H_y^{\text{inc}}, \quad (29)$$

where α_{ee}^{eff} and α_{mm}^{eff} are referred as the effective electric and magnetic polarizabilities of the array. By substituting Eqs. 28 and 29 into Eq. 26 and Eq. 27, the reflection and transmission coefficients of the array read

$$r = \frac{E_x^r}{E_x^{\text{inc}}} = \frac{ik}{2\Lambda^2 \Delta_{ee} \Delta_{mm}} (\alpha_{ee} - \alpha_{mm}), \quad (30)$$

$$\begin{aligned} t = \frac{E_x^t}{E_x^{\text{inc}}} &= 1 + \frac{ik}{2\Lambda^2 \Delta_{ee} \Delta_{mm}} [\alpha_{ee} + \alpha_{mm} \\ &\quad - \alpha_{ee} \alpha_{mm} (\beta_{ee} + \beta_{mm})], \end{aligned} \quad (31)$$

where $\Delta_{ee} = 1 - \alpha_{ee}\beta_{ee}$ and $\Delta_{mm} = 1 - \alpha_{mm}\beta_{mm}$. Note that $\beta_{ee} = \beta_{mm}$. Finally, the absorption is found as^{15,21,37}

$$\begin{aligned} A &= 1 - |r|^2 - |t|^2 \\ &= 1 - |r_{ee} - r_{mm}|^2 - |1 + r_{ee} + r_{mm}|^2, \end{aligned} \quad (32)$$

where $r_{ee} = \frac{ik}{2\Lambda^2} \alpha_{ee}^{\text{eff}}$ and $r_{mm} = \frac{ik}{2\Lambda^2} \alpha_{mm}^{\text{eff}}$. It can be shown that the maximum absorption occurs when

$$r_{ee} = r_{mm} = -\frac{1}{2} \Rightarrow \alpha_{ee}^{\text{eff}} = \alpha_{mm}^{\text{eff}}. \quad (33)$$

The above condition, i.e. $\alpha_{ee}^{\text{eff}} = \alpha_{mm}^{\text{eff}}$, is called balanced (Kerker) condition for the effective polarizabilities. Hence, the balanced condition for the individual polarizabilities is given by

$$\alpha_{ee} = \alpha_{mm} = \frac{1}{\beta_{ee} - \frac{ik}{\Lambda^2}}. \quad (34)$$

Note that the maximum absorption for an array of electric and magnetic dipoles (i.e. $A_{\max} = 1$) is twice the absorption that can be obtained from an array of only electric or magnetic dipoles. At the maximum absorption, the array will completely cancel the incident field in the forward direction without generating any backward wave, i.e. reflection [Fig. 8 (b)]. Moreover, the relation between the induced averaged electric and magnetic surface current densities in this case reads

$$\frac{J_y^m}{J_x^e} = \frac{E_x^{\text{inc}}}{E_x^{\text{inc}}/Z_0} = Z_0, \quad (35)$$

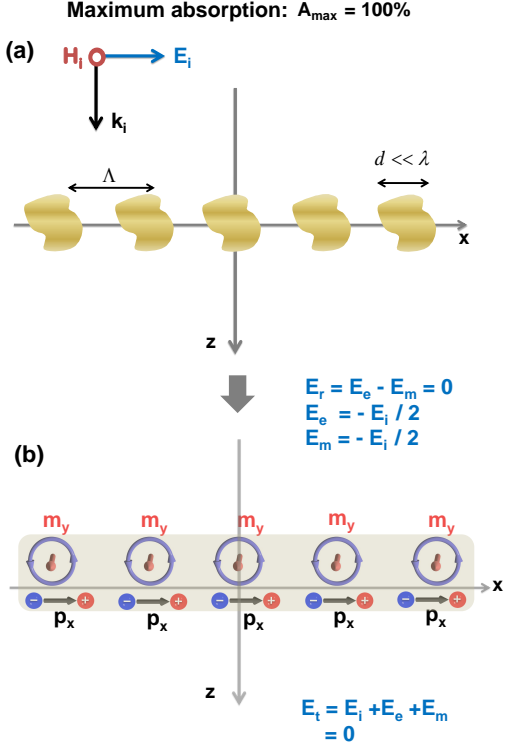


FIG. 8: (a) Geometry of an infinite periodic array of nanoantennas that support electric and magnetic dipole moments in a uniform host medium excited by a plane wave. The two-dimensional array is periodic in x-y plane. (b) show the radiated field by the average magnetic current density in the case of maximum absorption.

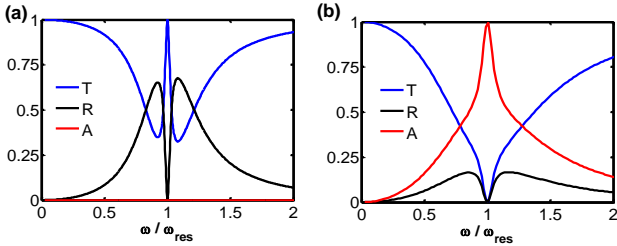


FIG. 9: (a) The transmission, reflection, and absorption as a function of normalized frequency for the lossless nanoantennas, i.e. $\gamma_{ee} = 0$ and $\gamma_{mm} = 0$. (b) The same plot as (a) for the complete absorption case that requires, i.e. $\gamma_{ee} = \frac{\alpha_{0ee}}{2\Lambda^2 c_0}$ and $\gamma_{mm} = \frac{\alpha_{0mm}}{2\Lambda^2 c_0}$. We assumed that the $\Lambda = \lambda_{\text{res}}/5$ and $\alpha_{0ee} = 8\alpha_{0mm} = \Lambda \times c_0^2$.

which simply means that the array is impedance matched with the embedding medium. The relation between electric and magnetic dipole moments of each nanoantenna in the total absorption regime, i.e. the so-called Kerker condition, is $p_x = m_y/c$.

In to order to understand the mechanism of total absorption for an array with both electric and magnetic dipole moments, let us assume that the dispersive char-

acteristics of the magnetic polarizability of the nanoantenna can be described by a Lorentzian line-shape (see Eq. 8 for the electric polarizability) that read as^{15,33}

$$\frac{1}{\alpha_{mm}} = \frac{\omega_{0mm}^2 - \omega^2 - i\omega\gamma_{mm}}{\alpha_{0mm}} - i\frac{k^3}{6\pi}, \quad (36)$$

where ω_{0mm} is the magnetic resonance angular frequency, γ_{0mm} is the Ohmic losses and α_{0mm} is the corresponding oscillator amplitude. By using Eq. 20 and the interparticle interaction constant, i.e. $\beta_{ee} = \beta_{mm} = \Re(\beta_{ee}) - i\frac{k^3}{6\pi} + i\frac{k}{2\Lambda^2}$, the reflection coefficient is given by

$$\begin{aligned} r &= \frac{ik}{2\Lambda^2} \left(\frac{1}{\frac{1}{\alpha_{ee}} - \beta_{ee}} - \frac{1}{\frac{1}{\alpha_{mm}} - \beta_{mm}} \right) \\ &= \frac{ik}{2\Lambda^2} \left[\frac{\alpha_{0ee}}{\omega_{0ee}'^2 - \omega^2 - i\omega \left(\gamma_{ee} + \frac{\alpha_{0ee}}{2\Lambda^2 c_0} \right)} - \frac{\alpha_{0mm}}{\omega_{0mm}'^2 - \omega^2 - i\omega \left(\gamma_{mm} + \frac{\alpha_{0mm}}{2\Lambda^2 c_0} \right)} \right] \\ &= \frac{ik}{2\Lambda^2} (\alpha_{ee}^{\text{eff}} - \alpha_{mm}^{\text{eff}}), \end{aligned} \quad (37)$$

where $\omega_{0mm}' = \omega_{0mm} - \Re(\beta_{mm})\alpha_{0mm}$ and $\omega_{0ee}' = \omega_{0ee} - \Re(\beta_{ee})\alpha_{0ee}$ are the resonance frequencies of the electric and magnetic dipoles in the array, respectively. The transmission coefficient correspondingly reads as

$$t = 1 + \frac{ik}{2\Lambda^2} (\alpha_{ee}^{\text{eff}} + \alpha_{mm}^{\text{eff}}).$$

Let us first consider a lossless metasurface. We assume that $\omega_{0ee} = \omega_{0mm} = \omega_{\text{res}}$. When the dipole nanoantennas in the array are lossless, i.e. $\gamma_{ee} = \gamma_{mm} = 0$, the transmission, reflection, and absorption as a function of normalized frequency are shown in Fig. 9 (a). In this case, the transmission possesses similar features to structures known in the context of electromagnetically induced transparency (EIT)⁵⁷. The array shows zero absorption and the reflection vanishes at the resonance frequency.

Next, we consider the case of maximum absorption (known as critical coupling). In this case, the Ohmic losses for the electric and magnetic dipoles are $\gamma_{ee} = \frac{\alpha_{0ee}}{2\Lambda^2 c_0}$, $\gamma_{mm} = \frac{\alpha_{0mm}}{2\Lambda^2 c_0}$, respectively. Figure 9 (b) depicts the spectral dependency of the optical coefficients in such situation. At the resonance frequency, we observe total absorption. Indeed, one achieves the electromagnetically induced absorption (EIA) by proper tuning of the electric and magnetic dipole moments⁵⁸. Several geometries have been proposed to achieve total absorption based on balanced electric and magnetic moments^{5,6,37,38,55,56,59}.

Besides the discussed scenario to obtain the total absorption in an array of dipole particles, there are other alternatives which exploit metasurfaces with either electric or magnetic responses while taking the advantage of

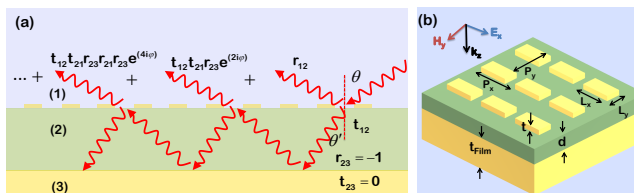


FIG. 10: (a) Asymmetric Fabry-Perot cavity model for a perfect absorber in the far-field interference scheme. (b) Schematic of the investigated perfect absorber. The geometrical parameters of the structure are: $t_{\text{Film}} = 300$ nm, $d = 20 - 1500$ nm, $L_x = 400$ nm, $L_y = 100$ nm, $P_x = P_y = 500$ nm and $t = 20$ nm.

a back reflector in their design which is the topic of the rest of this review study.

Next, we focus on this alternative approach to enhance the absorption of an array of electric dipole moment on top of a reflecting ground plane. As we will see, this alternative also allows to fully suppress the transmission while canceling out the reflection at the same time.

V. ASYMMETRIC FABRY-PEROT CAVITY AND PERFECT ABSORBERS

In the previous section, we have shown that the absorption of an array of rectangular nanopatches is limited to 50 percent. Note that this is a universal limitation as long as the nanopatches can be described by an electric dipole moment only, i.e. all higher order multipoles are negligible. One of the simplest and practical approaches to enhance the absorption is to use a metallic ground plate in order to suppress the transmission [Fig. 10 (a)]. In fact, complete light absorption occurs when the reflection goes to zero ($R = 0$) since the transmission is zero ($T = 0$) (due to the thick metallic ground plate). In order to achieve zero reflection, the dielectric spacer that separates the nanopatches from the ground plate should be properly tuned such that the directly reflected light at the nanopatch array interferes destructively with the light that experiences multiple reflections in the layered system [Fig. 10 (a)]. In the following, we will show that the optical response of the structure can be fully explained by a simple Fabry-Perot model. This model is only valid for considerably thick dielectric spacers when the effects of near-field coupling between ground plate and nanopatch array is negligible.

A. Theory of ground-back perfect absorption of electrically resonant sheets

The investigated perfect absorber consists of a metasurface on top of a metallic ground plate separated by a thick dielectric spacer [Fig. 10 (a)]. To simplify the structure and also to provide a physical explanation, we

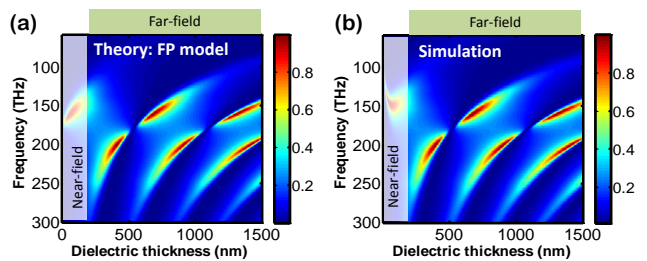


FIG. 11: (a) and (b) Theoretical and simulated absorption spectra as a function of the frequency and the dielectric thickness (d) of the spacer for a gold nanopatch based perfect absorber at normal incidence.

consider the structure as an asymmetric Fabry-Perot cavity with two mirrors, i.e., the metallic ground plate as the bottom mirror and the array of nanoantennas as the top mirror. By using Airy's formula, the total reflection and transmission coefficients read⁶⁰⁻⁶²:

$$r = r_{12} + r_m = r_{12} + \frac{t_{12}t_{21}r_{23}e^{(2i\varphi)}}{1 - r_{21}r_{23}e^{(2i\varphi)}}, \quad (38)$$

$$t = \frac{t_{12}t_{23}e^{(2i\varphi)}}{1 - r_{21}r_{23}e^{(2i\varphi)}}, \quad (39)$$

where t_{12} , t_{21} , r_{12} , r_{21} , r_{23} are complex-valued reflection and transmission coefficients at both interfaces, $\varphi = k_0 n d \cos \theta'$ is the phase accumulated upon a single cavity transfer, k_0 is the free space wavenumber, n is the refractive index of the dielectric spacer, and d is its thickness. A full wave simulation is used to calculate the reflection and transmission coefficients (r_{12} , t_{12} , r_{21} , and t_{21}) where the array of nanoantennas is assumed to be sandwiched between two semi-infinite half-spaces, i.e. air and dielectric and is illuminated by a linearly polarized incident plane wave either from the top air or from the bottom dielectric⁶¹.

As already mentioned, a perfect absorption is achievable if the reflection as well as transmission of the structure vanishes. The transmission of the structure is totally suppressed in any case, i.e. $T = |t| = 0$ due to sufficiently thick metallic ground plate (i.e. $t_{23} = 0$). To achieve total absorption ($A = 1 - T - R \simeq 1$) the reflection should be simultaneously zero ($R = |r|^2 = |r_{12} + r_m|^2 \simeq 0$). The reflection is the sum of the direct reflection coefficient r_{12} and the multiple reflection coefficient r_m [as sketched in Fig. 10 (a)]. Therefore, in the far-field scheme, the condition of the perfect absorption reads

$$r_{12} = -r_m. \quad (40)$$

In the next subsection, we will show that the total absorption occurs whenever Eq. 40 is fulfilled.

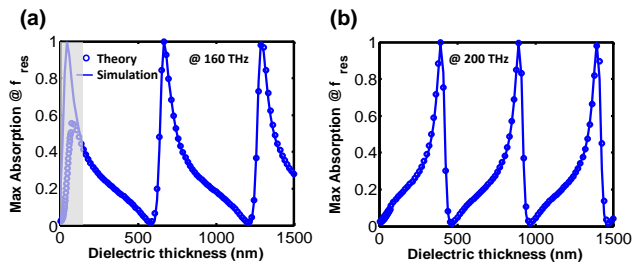


FIG. 12: Maximum absorption as a function of the thickness of the dielectric spacer calculated from the semi-analytical approach and from full wave simulations for two different frequencies at 160 THz (a) and at 200 THz (b), respectively.

B. Array of nanopatches on top of a metallic ground plate

The schematic view of the investigated perfect absorber is depicted in Fig. 10 (b). It consists of an array of rectangular gold nanopatches on top of a metallic ground plate separated by a thick dielectric spacer. The structure is periodic in x and y directions and the periods are $P_x = P_y = 500$ nm. The refractive index of the dielectric spacer is $n = \sqrt{\epsilon_d} = 1.5$. To explore the underlying physics of the investigated perfect absorber, we calculated the absorption A as a function of the thickness of the dielectric spacer d and the frequency [Fig. 11 (b)]. The dielectric spacer is varied from 20 – 1500 nm. To be able to compare it with the Fabry-Perot model, the simulated result is divided into two distinct parts, namely, far-field and near-field [Fig. 11 (a) and (b)]. The numerical result shows that the perfect absorption ($A = 1$) can be achieved for various dielectric spacer thicknesses d , periodically spaced around a frequency of operation. Moreover, the resonance frequency of maximum absorption is slightly changing for different dielectric spacer. Note that the hybridization of the localized eigenmode of the gold nanopatches with the Fabry-Perot resonance of the cavity can be clearly seen in Fig. 11 (a) and (b). This leads to a strong Rabi splitting and avoid crossing [Fig. 11 (a) and (b)].

The absorption spectra as a function of the dielectric spacer thickness d and resonance frequency is calculated by using the Airy's formula which shows similar behavior compared to the simulated results [Fig. 11 (a) and (b)]. As already highlighted, the analytical result does not predict the simulated result for thin dielectric spacers due to the strong coupling between nanopatches and the metallic ground plate. This can be better seen in Fig. 12 for two different resonance frequencies 160 THz (a) and 200 THz (b). The absorption is shown at those discrete frequencies as a function of the thickness of the dielectric spacer.

The analytical and numerical results are displayed in the same figure [Fig. 12 (a) and (b)] for comparison. For thick dielectric spacers, i.e. $d > 250$ nm, there is a perfect

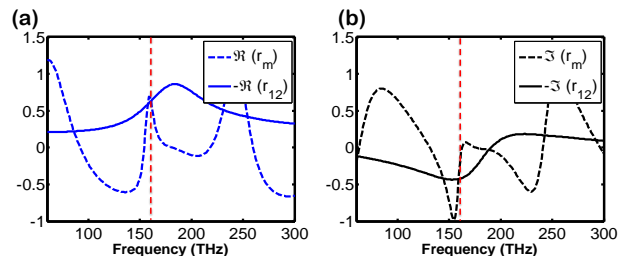


FIG. 13: (a) and (b) Real and imaginary parts of direct reflection coefficient (r_{12}) as well as multiple reflection coefficient (r_m) with dielectric thickness $d = 370$ nm. The red dashed lines represent the crossing point when real and imaginary parts of reflection coefficients have the same magnitude but opposite sign, i.e. $r_{12} = -r_m$.

agreement between the numerical and analytical results. However, for thin dielectric spacers, there is a huge deviation due to strong coupling between the metallic ground plate and the nanopatches. This has been investigated in detail in Refs. 59,63. In order to fully understand the absorption mechanism in the investigated structure, the real and imaginary parts of the direct reflection coefficient r_{12} and the multiple reflection coefficient r_m are calculated at the resonance frequency $f = 160$ THz for a spacer thickness $d = 370$ nm [Fig. 13 (a) and 13 (b)]. The total reflection coefficient is completely suppressed, i.e. $r = r_{12} + r_m = 0$, due to the destructive interference between both the reflection coefficients r_m and r_{12} , i.e. $r_{12} = -r_m$. Therefore, the absorption reaches nearly 100 percent for the investigated frequency.

VI. CONCLUSIONS

We have presented a review where by analytical means the universal limitation on the scattering/absorption cross section of a dipolar nanoantenna that supports an electric and/or a magnetic response was studied. We have provided a concise theoretical review that shows that a metasurface made of nanoantennas that sustain only either electric or magnetic dipole moments maximally absorbs 50 percent of the impinging light. To overcome this limitation, we have theoretically revisited two known alternatives to obtain a perfect absorber. One of them was established on the use of dipolar nanoantennas that simultaneously support both electric and magnetic responses whereas the other was based on a periodic array of electrically/magnetically resonant nanoantennas on top of a reflector. Moreover, for the second alternative, we have applied a simple semi-analytical approach based on an asymmetric Fabry-Perot model in order to investigate the optical responses of such a perfect absorber. The underlying mechanism of the total absorption is fully explained by destructive interference. We have provided a laconic explanation of underlying mechanism of the maximum absorption in each study case.

By providing a useful tutorial, the goal of the present work has been to bring about a correct physical insight in understanding the scattering/absorption phenomena both in the level of an individual meta-atom and also in the level of many inclusions of meta-atoms composing a metasurface. We believe that the current review would be helpful to a wide range of audience both in the junior and senior levels due to the concise presentation manner.

VII. ACKNOWLEDGMENTS

R.A. would like to acknowledge financial support from the Max Planck Society.

Appendix A: Derivation of scattered and extinct power for an electric dipole

Here we present a derivation for the scattered and extinct power shown in Eqs. (2) and (4) for an electrically dipolar polarizable particle when excited by an electromagnetic field. We assume that the particle contains only electric dipole moment, while similar expression may be derived for a magnetic dipole moment.

From the Poynting theorem²⁸, we have

$$\begin{aligned} \int_V \nabla \cdot (\mathcal{E}_{\text{tot}} \times \mathcal{H}_{\text{tot}}) dv &= - \int_V \mathcal{J} \cdot \mathcal{E}_{\text{tot}} dv \\ &- \int_V \mathcal{E}_{\text{tot}} \cdot \frac{\partial \mathcal{D}}{\partial t} dv \quad \text{Poynting1} \\ &- \int_V \mathcal{H}_{\text{tot}} \cdot \frac{\partial \mathcal{B}}{\partial t} dv, \end{aligned} \quad (\text{A1})$$

where \mathcal{E}_{tot} and \mathcal{H}_{tot} are the time varying *total* electric and magnetic fields while \mathcal{D} and \mathcal{B} are the electric displacement vector and magnetic induction, respectively, and \mathcal{J} is a current distribution in volume V . Considering the time harmonic fields with the time dependence $e^{-i\omega t}$ (i.e., the relation between the time harmonic fields is considered to be $\mathcal{A} = \Re\{\mathbf{A}e^{-i\omega t}\}$), the Poynting theorem reads (after averaging over a time cycle)

$$\begin{aligned} \int_V \nabla \cdot \frac{1}{2} \Re\{\mathbf{E}_{\text{tot}} \times \mathbf{H}_{\text{tot}}^*\} dv &= - \int_V \frac{1}{2} \Re\{\mathbf{J}^* \cdot \mathbf{E}_{\text{tot}}\} dv \\ &- \frac{\omega}{2} \int_V \text{Im}\{\mathbf{E}_{\text{tot}}^* \cdot \mathbf{D}\} dv \quad \text{PoyntTime} \\ &- \frac{\omega}{2} \int_V \text{Im}\{\mathbf{H}_{\text{tot}}^* \cdot \mathbf{B}\} dv. \end{aligned} \quad (\text{A2})$$

Considering a non-conductive, non-magnetic particle with only electrical properties; we have $\mathbf{J}^* \cdot \mathbf{E}_{\text{tot}} = 0$, $\mathbf{D} = \epsilon_0 \mathbf{E}_{\text{tot}} + \mathbf{P}$, and $\mathbf{B} = \mu_0 \mathbf{H}_{\text{tot}}$. Substituting these

quantities into PoyntTime, we reach at

$$\frac{1}{2} \int_V \nabla \cdot \text{Re}\{\mathbf{E}_{\text{tot}} \times \mathbf{H}_{\text{tot}}^*\} dv = \frac{\omega}{2} \int_V \text{Im}\{\mathbf{P}^* \cdot \mathbf{E}_{\text{tot}}\} dv. \quad \text{PoyntTime1} \quad (\text{A3})$$

The left hand side of Eq. PoyntTime1 is the total power going out of a surface embedding volume V which contains the particle, while the right hand side is the negative of the absorbed power since the absorbed power is going into the surface S of volume V (the work done by the field on the dipolar particle). Therefore, the absorbed power by one dipolar particle reads

$$P_{\text{abs}} = -\frac{\omega}{2} \text{Im}\{\mathbf{p}^* \cdot \mathbf{E}_{\text{tot}}\}, \quad \text{ABS} \quad (\text{A4})$$

since $\mathbf{P} = \int \mathbf{p} dv$. The electric field in $\hat{\mathbf{A}}$ is the total field at the position of the particle, which is the contribution of the local field and the scattered field by the dipole; i.e.,

$$\mathbf{E}_{\text{tot}} = \mathbf{E}_{\text{loc}} + \mathbf{E}_{\text{sca}}. \quad \text{tot} \quad (\text{A5})$$

Since we have one particle, then the local field is also the excitation field; i.e., $\mathbf{E}_{\text{loc}} = \mathbf{E}_{\text{inc}}$, and plugging tot into $\hat{\mathbf{A}}$ the absorbed power reads

$$\begin{aligned} P_{\text{abs}} &= -\frac{\omega}{2} \text{Im}\{\mathbf{p}^* \cdot \mathbf{E}_{\text{tot}}\} \\ &= -\frac{\omega}{2} \text{Im}\{\mathbf{p}^* \cdot \mathbf{E}_{\text{inc}}\} - \frac{\omega}{2} \text{Im}\{\mathbf{p}^* \cdot \mathbf{E}_{\text{sca}}\}. \end{aligned} \quad \text{ABSEXT} \quad (\text{A6})$$

Let us now calculate the second part of the right hand side of Eq. $\hat{\mathbf{A}}$, i.e., $\frac{\omega}{2} \text{Im}\{\mathbf{p}^* \cdot \mathbf{E}_{\text{sca}}\}$. The scattered electric field by a dipole reads²⁸

$$\begin{aligned} \mathbf{E}_{\text{sca}} &= \frac{e^{ikr}}{4\pi\epsilon_0} \left[(\mathbf{n} \times \mathbf{p}) \times \mathbf{n} \frac{k^2}{r} \right. \\ &\left. + [3\mathbf{n}(\mathbf{n} \cdot \mathbf{p}) - \mathbf{p}] \left(\frac{1}{r^3} - \frac{ik}{r^2} \right) \right], \end{aligned} \quad \text{dipoleScat} \quad (\text{A7})$$

then, we inner product both sides by \mathbf{p}^* to obtain

$$\begin{aligned} \mathbf{p}^* \cdot \mathbf{E}_{\text{sca}} &= \frac{e^{ikr}}{4\pi\epsilon_0} \left[\mathbf{p}^* \cdot [(\mathbf{n} \times \mathbf{p}) \times \mathbf{n}] \frac{k^2}{r} \right. \\ &\left. + [3(\mathbf{n} \cdot \mathbf{p}^*)(\mathbf{n} \cdot \mathbf{p}) - |\mathbf{p}|^2] \left(\frac{1}{r^3} - \frac{ik}{r^2} \right) \right]. \end{aligned} \quad \text{eqT} \quad (\text{A8})$$

Next, if we use the identity $\mathbf{p}^* \cdot [(\mathbf{n} \times \mathbf{p}) \times \mathbf{n}] = |\mathbf{p}|^2 - (\mathbf{n} \cdot \mathbf{p}^*)(\mathbf{n} \cdot \mathbf{p})$ in Eq. eqT, the result reads

$$\begin{aligned} \mathbf{p}^* \cdot \mathbf{E}_{\text{sca}} &= \frac{e^{ikr}}{4\pi\epsilon_0} \left([|\mathbf{p}|^2 - (\mathbf{n} \cdot \mathbf{p}^*)(\mathbf{n} \cdot \mathbf{p})] \frac{k^2}{r} \right. \\ &\left. + [3(\mathbf{n} \cdot \mathbf{p}^*)(\mathbf{n} \cdot \mathbf{p}) - |\mathbf{p}|^2] \left(\frac{1}{r^3} - \frac{ik}{r^2} \right) \right). \end{aligned} \quad \text{eqT1} \quad (\text{A9})$$

Now, we expand the exponential term $e^{ikr} = 1 + ikr - k^2 r^2/2 - ik^3 r^3/6 + \dots$ in Eq. eqT1, and take the imaginary

parts of both sides and then take their limits at $r \rightarrow 0$, (i.e., at the position of the particle). The result reads

$$\begin{aligned} \text{Im}\{\mathbf{p}^* \cdot \mathbf{E}_{\text{sca}}\}_{r \rightarrow 0} &= \frac{k^3}{4\pi\epsilon_0} ([|\mathbf{p}|^2 - (\mathbf{n} \cdot \mathbf{p}^*)(\mathbf{n} \cdot \mathbf{p})] \\ &+ \frac{1}{3} [3(\mathbf{n} \cdot \mathbf{p}^*)(\mathbf{n} \cdot \mathbf{p}) - |\mathbf{p}|^2]). \end{aligned} \quad \text{eqT111} \quad (\text{A10})$$

and when simplified to

$$\text{Im}\{\mathbf{p}^* \cdot \mathbf{E}_{\text{sca}}\}_{r \rightarrow 0} = \frac{k^3}{6\pi\epsilon_0} |\mathbf{p}|^2. \text{Scat1} \quad (\text{A11})$$

If we simply substitute $\hat{\text{Scat1}}$ into $\hat{\text{A}}$, we reach at

$$P_{\text{abs}} = -\frac{\omega}{2} \text{Im}\{\mathbf{p}^* \cdot \mathbf{E}_{\text{inc}}\} - \frac{\omega k^3}{12\pi\epsilon_0} |\mathbf{p}|^2. \text{ABSSCA} \quad (\text{A12})$$

The second term of the right hand side in $\hat{\text{A}}$, equals the negative of the scattered power by an electric dipole, [see Eq. (2)]. Therefore, one may simply rewrite Eq. $\hat{\text{A}}$ as

$$P_{\text{ext}} = -\frac{\omega}{2} \text{Im}\{\mathbf{p}^* \cdot \mathbf{E}_{\text{inc}}\} = P_{\text{abs}} + P_{\text{scat}}. \text{EXTABSSCA} \quad (\text{A13})$$

P_{ext} as discussed in Eq. (4) is called the extinct power and is the sum of the absorbed and the scattered powers by the dipole. Notice, due to the duality of the electric and magnetic fields/currents in the Maxwell's equations, similar formulations can be provided for a magnetic dipole with the same procedure.

-
- ¹ B. A. Munk, *Frequency selective surfaces: theory and design*. John Wiley & Sons (2005).
 - ² W. Dallenbach and W. Kleinsteuber, "Reflection and absorption of decimeter-waves by plane dielectric layers," *Hochfreq. u Elektroak*, **51**, 152 (1938).
 - ³ W. W. Salisbury, "Absorbent body for electromagnetic waves," (1952). US Patent 2,599,944.
 - ⁴ N. Engheta, "Thin absorbing screens using metamaterial surfaces," in *Antennas and Propagation Society International Symposium, 2002. IEEE*, **2**, 392 (2002).
 - ⁵ N. Landy, S. Sajuyigbe, J. Mock, D. Smith, and W. Padilla, "Perfect metamaterial absorber," *Phys. Rev. Lett.*, **100**, 207402 (2008).
 - ⁶ C. M. Watts, X. Liu, and W. J. Padilla, "Metamaterial electromagnetic wave absorbers," *Adv. Mater.*, **24**, OP98 (2012).
 - ⁷ Y. Ra'di, V. S. Asadchy and S. A. Tretyakov "Total Absorption of Electromagnetic Waves in Ultimately Thin Layers," *IEEE Trans. Antennas. Propag.*, **61**, 4606 (2013).
 - ⁸ N. Liu, H. Guo, L. Fu, S. Kaiser, H. Schweizer, and Giessen, "Plasmon hybridization in stacked cut-wire metamaterials," *Adv. Mat.*, **19**, 3628, (2007).
 - ⁹ Y. Avitzour, Y. A. Urzhumov, and G. Shvets, "Wide-angle infrared absorber based on a negative-index plasmonic metamaterial," *Phys. Rev. B*, **79**, 045131 (2009).
 - ¹⁰ N. Liu, M. Mesch, T. Weiss, M. Hentschel, and H. Giessen, "Infrared perfect absorber and its application as plasmonic sensor," *Nano Lett.*, **10**, 2342 (2010).
 - ¹¹ M. Pu, C. Hu, M. Wang, C. Huang, Z. Zhao, C. Wang, Q. Feng, and X. Luo, "Design principles for infrared wide-angle perfect absorber based on plasmonic structure," *Opt. Expr.*, **19**, 17413, (2011).
 - ¹² J. R. Piper, and S. Fan, "Total Absorption in a Graphene Monolayer in the Optical Regime by Critical Coupling with a Photonic Crystal Guided Resonance," *ACS Photonics*, **1**, 347 (2014).
 - ¹³ L. Huang, D. R. Chowdhury, S. Ramani, M. T. Reiten, S.-N. Luo, A. J. Taylor, and H.-T. Chen, "Experimental demonstration of terahertz metamaterial absorbers with a broad and flat high absorption band," *Opt. Lett.*, **37**, 154 (2012).
 - ¹⁴ R. Alaee, C. Menzel, C. Rockstuhl, and F. Lederer, "Perfect absorbers on curved surfaces and their potential applications," *Opt. Express*, **20**, 18370 (2012).
 - ¹⁵ M. Albooyeh, D. Morits, and S. Tretyakov, "Effective electric and magnetic properties of metasurfaces in transition from crystalline to amorphous state," *Phys. Rev. B*, **85**, 205110 (2012).
 - ¹⁶ K. Aydin, V. E. Ferry, R. M. Briggs, and H. A. Atwater, "Broadband polarization-independent resonant light absorption using ultrathin plasmonic super absorbers," *Nat Commun*, **2**, 517 (2011).
 - ¹⁷ C. Hu, Z. Zhao, X. Chen, and X. Luo, "Realizing near-perfect absorption at visible frequencies," *Opt. Express*, **17**, 11039 (2009).
 - ¹⁸ U. Huebner, E. Pshenay-Severin, R. Alaee, C. Menzel, M. Ziegler, C. Rockstuhl, F. Lederer, T. Pertsch, H.-G. Meyer, and J. Popp, "Exploiting extreme coupling to realize a metamaterial perfect absorber," *Microelectron Eng.*, **111**, 110 (2013).
 - ¹⁹ The content of this paper has been published in Ph.D. thesis, R. Alaee, "Optical Nanoantennas and Their Use as Perfect Absorbers" (2015), DOI(KIT): 10.5445/IR/1000051727.
 - ²⁰ S. A. Maier, *Plasmonics: Fundamentals and Applications*. Springer (2007).
 - ²¹ S. Tretyakov, *Analytical modeling in applied electromagnetics*. Artech House (2003).
 - ²² C. J. Foot, *Atomic Physics*. Oxford University Press, New York (2005).
 - ²³ D. H. Kwon and D. M. Pozar, "Optimal Characteristics of an Arbitrary Receive Antenna," *IEEE Trans. Antennas. Propag.*, **57**, 3720 (2009).
 - ²⁴ Z. Ruan and S. Fan, "Superscattering of light from sub-wavelength nanostructures," *Phys. Rev. Lett.*, **105**, 013901 (2010).
 - ²⁵ L. Novotny and B. Hecht, *Principles of nano-optics* (Cambridge university press (2012)).
 - ²⁶ S. Tretyakov, "Maximizing absorption and scattering by dipole particles," *Plasmonics*, **9**, 935 (2014).
 - ²⁷ O. D. Miller, A. G. Polimeridis, M. T. H. Reid, C. W. Hsu, B. G. DeLacy, J. D. Joannopoulos, M. Soljačić, and

- S. G. Johnson, "Fundamental limits to optical response in absorptive systems," *Opt. Express*, **24**, 3329 (2016).
- ²⁸ J. D. Jackson, *Classical Electrodynamics*. Wiley, 3rd ed. (1998).
- ²⁹ D. R. H. Craig F. Bohren, *Absorption and Scattering of Light by Small Particles*. Wiley-VCH (1998).
- ³⁰ D. S. Filonov, A. E. Krasnok, A. P. Slobozhanyuk, P. V. Kapitanova, E. A. Nenasheva, Y. S. Kivshar, and P. A. Belov, "Experimental verification of the concept of all-dielectric nanoantennas," *Appl. Phys. Lett.*, **100**, 201113 (2012).
- ³¹ Z. Ruan and S. Fan, "Design of subwavelength superscattering nanospheres," *Appl. Phys. Lett.*, **98**, 043101 (2011).
- ³² C. F. Bohren, "How can a particle absorb more than the light incident on it?," *Am. J. Phys.*, **51**, 323 (1983).
- ³³ J. E. Sipe and J. V. Kravendonk, "Macroscopic electromagnetic theory of resonant dielectrics," *Phys. Rev. A*, **9**, 1806 (1974).
- ³⁴ R. Alaei, and C. Rockstuhl, and I. Fernandez-Corbaton "An electromagnetic multipole expansion beyond the long-wavelength approximation," *Opt. Commun.*, **407**, 17 (2018).
- ³⁵ P. B. Johnson and R. W. Christy, "Optical constants of the noble metals," *Phys. Rev. B*, **6**, 4370 (1972).
- ³⁶ C. Multiphysics, "4.3 user's guide," (2012).
- ³⁷ R. Alaei, M. Albooyeh, M. Yazdi, N. Komjani, C. Simovski, F. Lederer, and C. Rockstuhl, "Magnetolectric coupling in nonidentical plasmonic nanoparticles: Theory and applications," *Phys. Rev. B*, **91**, 115119 (2015).
- ³⁸ M. Albooyeh and C. R. Simovski, "Huge local field enhancement in perfect plasmonic absorbers," *Optics Express*, **20**, 21888 (2012).
- ³⁹ M. Darvishzadeh-Varcheie, C. Guclu, and F. Capolino, "Magnetic Nanoantennas Made of Plasmonic Nanoclusters for Photoinduced Magnetic Field Enhancement," *Phys. Rev. Applied*, **8**, 024033 (2017).
- ⁴⁰ S. D. Swiecicki and J. E. Sipe, "Surface-lattice resonances in two-dimensional arrays of spheres: Multipolar interactions and a mode analysis," *Phys. Rev. B*, **95**, 195406 (2017).
- ⁴¹ M. Husnik, M. W. Klein, N. Feth, M. Konig, J. Niegemann, K. Busch, S. Linden, and M. Wegener, "Absolute extinction cross-section of individual magnetic split-ring resonators," *Nat. Photon*, **2**, 614 (2008).
- ⁴² M. Husnik, S. Linden, R. Diehl, J. Niegemann, K. Busch, and M. Wegener, "Quantitative experimental determination of scattering and absorption cross-section spectra of individual optical metallic nanoantennas," *Phys. Rev. Lett.*, **109**, 233902 (2012).
- ⁴³ M. Husnik, J. Niegemann, K. Busch, and M. Wegener, "Quantitative spectroscopy on individual wire, slot, bow-tie, rectangular, and square-shaped optical antennas," *Opt. Lett.*, **38**, 4597 (2013).
- ⁴⁴ R. Alaei, M. Albooyeh, S. Tretyakov, and C. Rockstuhl, "Phase-change material-based nanoantennas with tunable radiation patterns," *Opt. Lett.*, **41**, 4099 (2016).
- ⁴⁵ A. Rahimzadegan, R. Alaei, I. Fernandez-Corbaton, and C. Rockstuhl, "Fundamental Limits of Optical Force and Torque," *Phys. Rev. B*, **95**, 035106 (2017).
- ⁴⁶ F. G. De Abajo, "Colloquium: Light scattering by particle and hole arrays," *Rev. Mod. Phys.*, **79**, 1267 (2007).
- ⁴⁷ N. J. Halas, S. Lal, W.-S. Chang, S. Link, and P. Nordlander, "Plasmons in strongly coupled metallic nanostructures," *Chem. Rev.*, **111**, 3913 (2011).
- ⁴⁸ C. Menzel, R. Alaei, E. Pshenay-Severin, C. Helgert, A. Chipouline, C. Rockstuhl, T. Pertsch, and F. Lederer, "Genuine effectively biaxial left-handed metamaterials due to extreme coupling," *Opt. Lett.*, **37**, 596 (2012).
- ⁴⁹ R. E. Collin, *Field theory of guided waves*. McGraw-Hill (1960).
- ⁵⁰ M. Yazdi and M. Albooyeh, "Analysis of metasurfaces at oblique incidence," *IEEE Trans. Antennas. Propag.*, **65**, 2397 (2017).
- ⁵¹ M. Idemen and A. H. Serbest, "Boundary conditions of the electromagnetic field," *Electron. Lett.*, **23**, 704 (1987).
- ⁵² C. L. Holloway, M. A. Mohamed, E. F. Kuester, and A. Dienstfrey, "Reflection and transmission properties of a metafilm: With an application to a controllable surface composed of resonant particles," *IEEE Trans. on Electromag. Comp.*, **47**, 853 (2005).
- ⁵³ M. Albooyeh, "Electromagnetic characterization of metasurfaces," PhD-Thesis (2015).
- ⁵⁴ M. Albooyeh, S. Tretyakov, and C. Simovski, "Electromagnetic characterization of bianisotropic metasurfaces on refractive substrates: General theoretical framework," *Annalen der Physik*, **528**, 721 (2016).
- ⁵⁵ M. Yazdi, M. Albooyeh, R. Alaei, V. Asadchy, N. Komjani, C. Rockstuhl, C. R. Simovski, and S. Tretyakov, "A bianisotropic metasurface with resonant asymmetric absorption," *IEEE Transactions on Antennas and Propagation*, **63**, 3004 (2015).
- ⁵⁶ Y. Ra'adi, C. R. Simovski, and S. A. Tretyakov, "Thin perfect absorbers for electromagnetic waves: Theory, design, and realizations," *Phys. Rev. Applied*, **3**, 037001 (2015).
- ⁵⁷ Y. Yang, and I.I Kravchenko, and D. P. Briggs, and J. Valentine, "All-dielectric metasurface analogue of electromagnetically induced transparency," *Nat Commun.*, **5**, 5753 (2014).
- ⁵⁸ R. Taubert, M. Hentschel, J. Kästel, and H. Giessen, "Classical analog of electromagnetically induced absorption in plasmonics," *Nano Lett.*, **12**, 1367 (2012).
- ⁵⁹ R. Alaei, C. Menzel, U. Huebner, E. Pshenay-Severin, S. Bin Hasan, T. Pertsch, C. Rockstuhl, and F. Lederer, "Deep-subwavelength plasmonic nanoresonators exploiting extreme coupling," *Nano Letters*, **13**, 3482 (2013).
- ⁶⁰ B. E. A. Saleh and M. C. Teich, *Fundamentals of Photonics*. Wiley Series in Pure and Applied Optics, Wiley-Interscience, 2nd ed. (2007).
- ⁶¹ R. Alaei, M. Farhat, C. Rockstuhl, and F. Lederer, "A perfect absorber made of a graphene micro-ribbon metamaterial," *Opt. Express*, **20**, 28017 (2012).
- ⁶² H.-T. Chen, "Interference theory of metamaterial perfect absorbers," *Opt. Express*, **20**, 7165 (2012).
- ⁶³ C. Ciraci, R. T. Hill, J. J. Mock, Y. Urzhumov, A. I. Fernández-Domínguez, S. A. Maier, J. B. Pendry, A. Chilkoti, and D. R. Smith, "Probing the ultimate limits of plasmonic enhancement," *Science*, **337**, 1072 (2012).